Theoret. Chim. Acta (Berl.) 43, 175–184 (1976)

THEORETICA CHIMICA ACTA

Moment Characterization of Localized Orbitals

Ede Kapuy and Cornelia Kozmutza

Quantum Theory Group, Physics Institute of the Technical University of Budapest, 1111 Budapest XI, Budafoki ut 8, Hungary

Michael E. Stephens

Centre de Mécanique Ondulatoire Appliquée, Paris, France

The parallel between orbital first and second electric moments and statistical first and second central moments is noted. Three measures of orbital spatial distribution in terms of their moments are proposed, and applied to the LMO's in a series of ten-electron hydrides. Consistent differences between bond and lone pair distributions are found. Using the statistical interpretation, for each LMO an "effective" solid angle around the central atom is postulated.

Key words: Localized molecular orbitals, electric moments of ~

1. Introduction

As is well known, single-determinantal wavefunctions of closed-shell atomic and molecular electronic eigenstates are invariant (except for a phase factor of modulus unity) under any unitary transformation of the orbitals. The transformation can be chosen to obtain localized molecular orbitals (LMO) from the canonical (CMO) set. A number of localization procedures have been proposed, differing only in the particular energetic or spatial criterion of localization chosen [1-5].

All the methods yield comparable results. Each LMO density is found to be relatively concentrated in some spatial region (but see [6]), and is expected to be determined mainly by that part (subsystem) of the molecule which occupies the given region plus its near environment, rather than by the whole system. As a consequence, the description of molecular electronic structure in terms of LMO's has several advantages:

1. The LMO's can be used to connect the orbital description with classical chemical concepts: bonds, unshared pairs and the like.
2. The comparison of the electronic structure of chemically related molecules is easier in the localized one-particle model because chemically identifiable structural units (functional groups) may be consistently described by more or less identical LMO's.
3. The LMO's of structurally related systems may be transferable, to a certain approximation, from one molecule to another. This makes it possible to use LMO's calculated for small molecules as building blocks in preliminary investigations of larger systems.

4. For extended systems, the localized description may be a better starting point if one wants to go beyond the independent-particle approximation.

The use of first and second moments of LMO densities for their characterization was introduced by Robb *et al.* [7]. A detailed analysis of the LMO's for a series of ten-electron systems has been done via a variant of their moment ellipsoid model [8]. In the present paper we investigate the further possibility of using the orbital first and second moments to characterize LMO's in statistical terms, through further analysis of the calculations on these molecules.

2. Characterization of Localized Orbitals by the First and Second Moments of Their Charge Distribution

The charge distributions of LMO's can be expressed in terms of their moments to any desired accuracy using the (infinite-order) multipole expansion technique.

The three first moments of the ith LMO, ϕ_i:

$$\langle u\rangle_i = \langle\phi_i | u | \phi_i\rangle, \qquad u = x, y, z \tag{1}$$

where x, y, z are the spatial coordinates of the electron, are the components of the orbital centroid-of-charge vector, $\langle \boldsymbol{r}\rangle_i$. The origin of $\langle \boldsymbol{r}\rangle_i$ is (conventionally) chosen at the nucleus of the central atom. The absolute value of $\langle \boldsymbol{r}\rangle_i$ is called the centroid length and denoted by $\langle r\rangle_i$.

The second moments are defined as:

$$\langle uv\rangle_i^0 = \langle\phi_i | uv | \phi_i\rangle, \qquad u, v = x, y, z. \tag{2}$$

As they depend on the origin of the coordinate system, we choose the explicit definition:

$$\langle uv\rangle_i = \langle\phi_i | [u - \langle u\rangle_i]\,[v - \langle v\rangle_i] | \phi_i\rangle, \qquad u, v = x, y, z \tag{3}$$

where the origin is taken to be the centroid-of-charge of the corresponding LMO. The higher moments can be defined in a similar way.

Expressions (3) are the components of a symmetrical second-order tensor which can be brought to diagonal form by a suitable rotation of the coordinate axes. The tensor is characterized by the diagonal elements (eigenvalues) $\langle x'^2\rangle$, $\langle y'^2\rangle$, $\langle z'^2\rangle$ of its diagonal form, and by the directions of the new coordinate axes.

These moments of a charge distribution can be related to the statistical moments of random variables. The orbital centroid vector is formally identical to the central first moment $M(\xi)$ of a random variable ξ with density function $p(x)$:

$$M(\xi) = \int_{-\infty}^{\infty} xp(x)\,dx. \tag{4}$$

Similarly, the definition of each diagonal element of the orbital second-moment tensor (3) is formally identical to that of the statistical central second moment, m_2:

$$m_2 = D^2(\xi) = \int_{-\infty}^{\infty} p(x)[x - M(\xi)]^2\,dx \tag{5}$$

where $D(\xi)$ is the standard deviation of ξ [9].

It is well known that for the standard deviation, $D(\xi)$, the following inequality holds (Bienaymé-Chebyshev theorem):

$$P(|\xi - M(\xi)| > \lambda D) \leqslant \frac{1}{\lambda^2}, \qquad \lambda \geqslant 1. \tag{6}$$

The expression on the left-hand side denotes the probability that $|\xi - M(\xi)|$ is larger than λ times the standard deviation. If we take $\lambda = 2$ as an example, then according to (6), the probability that ξ lies within the range $-2D(\xi) \leqslant \xi \leqslant 2D(\xi)$ is at least 0.75. For $0 \leqslant \lambda \leqslant 1$ the inequality remains valid but becomes trivial. When the probability function is Gaussian,

$$P(|\xi - M(\xi)| > D) = 0.3174.$$

Although inequality (6) is not very "sharp", it still gives some limiting value of the dispersion of random variable ξ, without knowing its distribution function explicitly. The same relation applies to the eigenvalues $\langle x'^2 \rangle_i, \langle y'^2 \rangle_i, \langle z'^2 \rangle_i$ of the LMO second-moment tensor, which are thus analogues of the statistical squared standard deviations. Hence, in principle the main features of the spatial extension of LMO's can be described by the first and second moments of their charge distribution. Depending on the information desired, more detailed knowledge may not be necessary.

3. Features of LMO First and Second Moments of Some Neutral Ten-Electron Systems

In all the calculations referred to in this paper, basis sets of $(13s7p/4s)$ Gaussians contracted to $[4s2p/2s]$ have been used. The bond distances and angles were fixed at the experimental equilibrium values of the neutral species [10]. Further details on the SCF, orbital localization and moment calculations may be found in [8] and [11].

3.1. First Moments

In all systems investigated, the length of the centroid vector, $\langle r \rangle$, was found to be larger for the bond pair LMO's than for the lone pair LMO's; their ratio is 1.61 for NH_3, and 1.60 for H_2O and HF. For systems of C_{2v} and C_{3v} symmetry, the centroid vectors of the bond LMO's do not point exactly towards the protons. However, the deviation is small: 0.6° for H_2O and 0.3° for NH_3, the angle between the centroid vectors being smaller than the corresponding valence angle in both cases. The angles between the three combinations of bond and lone pair centroid vectors are given in Table 1 (first part). It can be seen that the angles between two lone pair centroid vectors are consistently larger than between bond pair LMO vectors.

3.2. Second Moments

As noted above, the data contained in the LMO second-moment tensor is summarized in the three square roots of the eigenvalues, $\langle x'^2 \rangle, \langle y'^2 \rangle, \langle z'^2 \rangle$, of its diagonal form, identifiable as probability dispersions in the direction of the three axes, x', y', z', of the

Table 1. Characteristic angles (in degrees) of LMO first and second moments for a neutral series of ten-electron hydrides[a]

	Angles Between the Centroid Vectors			Deviation of the Major Dispersion Axis From the Centroid Vector	
	Bond–Bond	Bond–Lone	Lone–Lone	Bond	Lone
Ne	–	–	109.48	–	0.0
HF	–	105.8	112.9	0.0	6.4
H_2O	103.3	108.8	117.6	2.4	8.5
NH_3	106.1	112.7	–	3.2	0.0
CH_4	109.48	–	–	0.0	–

[a] Valence bond angles: H_2O (104.52), NH_3 (106.69).

rotated coordinate system required. For all molecules investigated, the eigenvalues were found to be doubly degenerate. In the symmetrical cases (all LMO's in Ne and CH_4, lone pair LMO in NH_3, and bond pair LMO in HF) the two minor values (denoted by $\langle y'^2\rangle^{1/2}$ and $\langle z'^2\rangle^{1/2}$) are equal to the accuracy of the orbital expansions. In all other cases (all LMO's in H_2O, bond pair LMO's in NH_3, and lone pair LMO's in HF) the relative difference between the two minor axes is at most 0.5%. The unique axis (x') of larger eigenvalue ($\langle x'^2\rangle$) coincides with the corresponding centroid vector only in the symmetrical cases. In all other cases, x' makes a non-zero angle with the centroid vector. This angle of deviation is largest for lone pair LMO's, but smaller than 10° in all cases (see Table 1, second part). The deviation angles, of the centroid vector, and of the principle dispersion axis, from the internuclear bond axes were consistently found to be of opposite sign.

In addition to the centroid length, by combining first- and second-moment data one can introduce three quantities characteristic of the various types (bond, lone pair) of LMO. One is the ratio of major and minor dispersions, $\langle x'^2\rangle_i^{1/2}/\langle y'^2\rangle_i^{1/2}$, which describes the deformation of the LMO from sphericity about its centroid. These values for the neutral species are given in Table 2 (second column).

Table 2. Characteristic measures of LMO first and second moments for a neutral series of ten-electron hydrides

	Centroid Length (in a.u.) $\langle r\rangle$		Major/Minor Dispersion Ratio $\langle x'^2\rangle^{1/2}/\langle y'^2\rangle^{1/2}$		Asymmetry $\langle r\rangle/\langle x'^2\rangle^{1/2}$		Effective Solid Angle (in steradians)	
	Bond	Lone	Bond	Lone	Bond	Lone	Bond	Lone
Ne	–	0.435	–	1.272	–	0.693	–	2.124
HF	0.831	0.521	1.496	1.242	0.930	0.709	1.181	2.131
H_2O	0.978	0.605	1.446	1.250	1.016	0.721	1.090	2.097
NH_3	1.148	0.713	1.385	1.221	1.117	0.750	1.007	2.038
CH_4	1.361	–	1.337	–	1.215	–	0.930	–

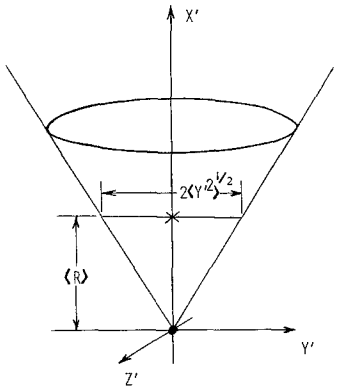

Fig. 1. Definition of the effective solid angle for a valence shell orbital. The heavy atom is indicated by a filled circle, the orbital centroid by a cross

The second is the ratio of centroid length to major dispersion, $\langle r_i\rangle/\langle x'^2\rangle_i^{1/2}$, the "asymmetry" of the LMO with respect to the central atom. When this ratio is zero, the orbital is symmetric (in the x'-direction) about the heavy atom, whatever the diffuseness of its density (measured by $\langle x'^2\rangle_i^{1/2}$). As the ratio increases, the orbital is characterized as having the principal amount of its density (roughly between $\pm\langle x'^2\rangle_i^{1/2}$ of its centroid) further from the heavy atom, which is not given by $\langle r\rangle_i$ alone.

Thirdly, in accordance with the meaning of the central second moments in probability theory (Sect. 2), one can define an "effective" orbial solid angle: the angular space around the central atom occupied predominantly by some one of the valence LMO's. As the deviation of the major dispersion axis from the corresponding centroid vector has been found to be less than 10° in the examples studied, the effective solid angle can be identified, approximately, with the solid angle subtended by a cone of semivertex angle $\arctan[\langle y'^2\rangle_i^{1/2}/\langle r\rangle_i]$, with vertex at the central nucleus and rotation axis in the direction of the centroid vector (see Fig. 1).

Taking into account the statistical meaning of the standard deviation, it should be emphasized that it is rather the relative magnitude, and not the absolute value, of the effective angle which is important. In the case of the H_2O molecule, the computed effective solid angles of its four valence LMO's are shown in Fig. 2a; the case of the NH_3 molecule is given in Fig. 2b. It can be seen that larger angular spaces are taken up by the lone pair LMO's than by the bonds. The effective solid angles for the neutral species studied are given in Table 2 (fourth column).

4. The Influence of Changes in Nuclear Charges on LMO Second Moments

As has been shown [6, 7], changes in the nuclear charges bring about systematic modifications in the distribution of the LMO densities, which are reflected also in their first and second moments.

On increasing the charge of the central nucleus and/or the number of protons, the total electronic cloud of the system contracts. Consistent with this observation, the measures of the radial spatial extensions of the component LMO's are also found to decrease. This variation in the centroid lengths for bond and lone pair LMO's for $O^{2-} \rightarrow H_4O^{2+}$

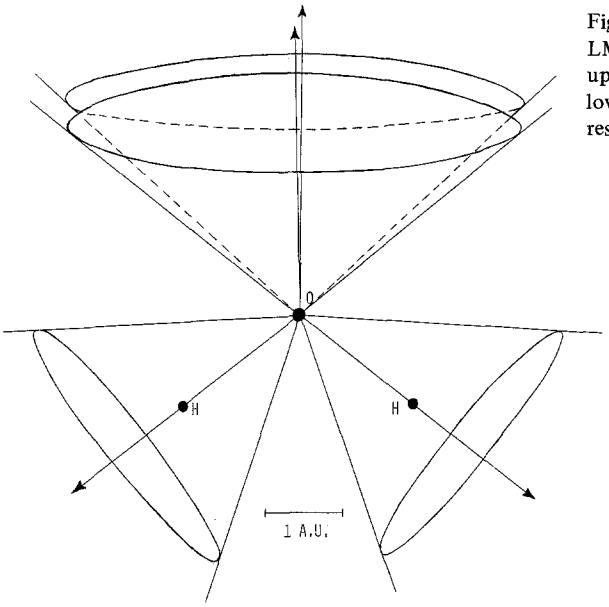

Fig. 2a. Effective solid angles for the LMO's of the H_2O molecule. The upper cones represent the lone, the lower ones the bond pair LMO's respectively

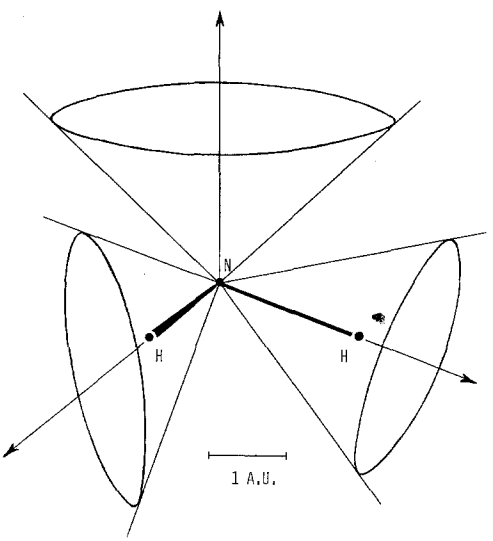

Fig. 2b. Spatial relation of valence orbital effective angles around the heavy atom in NH_3 (fourth cone, projecting behind the plane of the figure at lower left, not shown for clarity)

is shown in Fig. 3. For the neutral species, the corresponding values can be found in Table 2.

However, the rates of change of the individual components of the first and second moments are not uniform. So their various ratios may not vary monotonically for either the bond or lone pair LMO series. In Figs. 4 to 6 are shown the changes (with

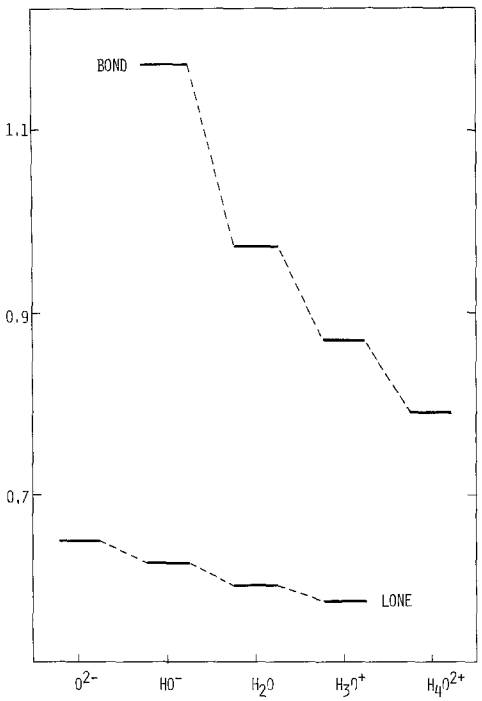

Fig. 3. Centroid length, $\langle r \rangle$, (in a.u.) for bond and lone pair LMO's in the molecular series $O^{2-} \rightarrow H_4O^{2+}$

increasing number of protons) of the characteristic properties proposed in Sect. 3, for the series $O^{2-} \rightarrow H_4O^{2+}$. The corresponding values for the neutral systems are given in Table 2.

The ratio of the dispersions, $\langle x'^2 \rangle_i^{1/2} / \langle y'^2 \rangle_i^{1/2}$, is given in Fig. 4. With increasing number of protons, this ratio decreases from 1.49 to 1.38 for bond pairs, and slowly increases from 1.23 to 1.26 for lone pairs. The gap between these ranges clearly differentiates the more spherical (around the centroid) lone pairs from the bond orbitals.

The asymmetry of the orbitals, $\langle r \rangle_i / \langle x'^2 \rangle_i^{1/2}$, decreases with increasing protonation within both bond (1.07 to 0.93) and lone pair (0.75 to 0.72) LMO series (see Fig. 5). The gap between the bond and lone pair ranges clearly illustrates the greater net displacement of the bond density from the central atom.

Finally, the effective solid angle changes very little for lone pair LMO's, varying between 2.03 and 2.10 steradians, but increases appreciably for bond LMO's from 0.97 to 1.33 steradians (see Fig. 6). Again there is a significant gap between bond and lone pair ranges. The consistently larger lone pair angle computed parallels the similar well known hypothesis of the VSEPR model of molecular structure [12].

These patterns of variation of the three proposed measures also hold for the C, N, F and Ne protonation series definable from the ensemble of ten-electron molecules studied. The gap between bond and lone pair ranges for each property persists in the neutral series of molecules as well (Table 2).

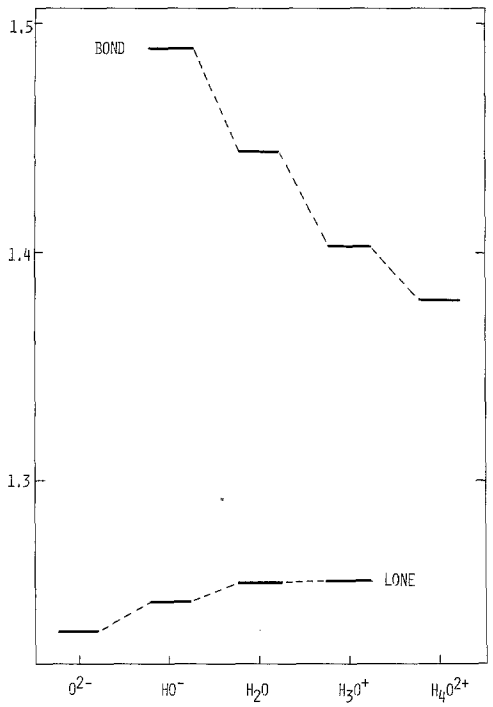

Fig. 4. Dispersion ratio, $\langle x'^2 \rangle_i^{1/2} / \langle y'^2 \rangle_i^{1/2}$, for bond and lone pair LMO's in the molecular series $O^{2-} \rightarrow H_4O^{2+}$

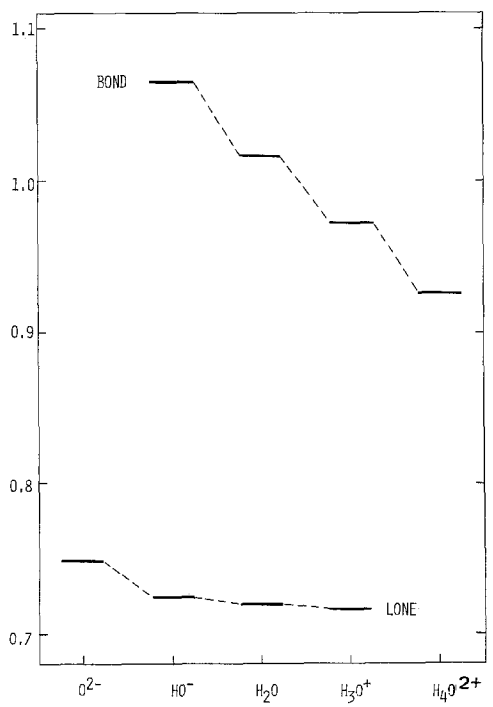

Fig. 5. Asymmetry, $\langle r \rangle_i / \langle x'^2 \rangle_i^{1/2}$, for bond and lone pair LMO's in the molecular series $O^{2-} \rightarrow H_4O^{2+}$

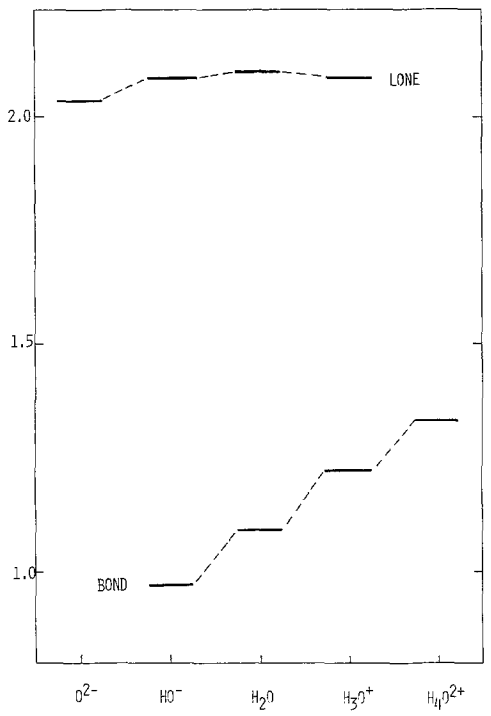

Fig. 6. Effective solid angle (in steradians) for bond and lone pair LMO's in the molecular series $O^{2-} \rightarrow H_4O^{2+}$

5. Conclusions

The parallel between orbital first and second electric moments and the statistical first and second central moments of random variables is underlined.

Three measures of orbital spatial distribution proposed here are shown to reveal consistent characteristic differences between bond and lone pair LMO's in a sample series of ten-electron hydrides. The empirical VSEPR model lone-bond subtended orbital angle postulate is shown to have a parallel in the statistical interpretation of LMO charge densities. The three measures together may yield a useful fashion of summarizing the information on molecular electronic structure provided by the LMO description.

It would be interesting to investigate the variation of these characteristics for extended systems, e.g. CH_3-CH_3, CH_3=NH_2, CH_3-OH, etc. This will form the subject of further study.

Acknowledgements. C. K. and M. E. S. wish to express their appreciation for the access to the facilities of the Centre de Mécanique Ondulatoire Appliquée, Paris, France, given them through its director, Professor R. Daudel, during these studies.

References

1. Edmiston, C., Ruedenberg, K.: Rev. Mod. Phys. **35**, 457 (1963); Edmiston, C., Ruedenberg, K.: J. Chem. Phys. **43**, S97 (1965)
2. Gilbert, T. L.: Molecular orbitals in chemistry, physics and biology, Löwdin, P. O., Pullman, B., Eds. New York: Academic Press 1964
3. Boys, S. F.: Quantum theory of atoms, molecules and the solid state, Löwdin, P. O., Ed. New York: Academic Press 1966
4. England, W., Salmon, L. S., Ruedenberg, K.: Topics Current Chem. **23**, 31 (1971)
5. Weinstein, H., Pauncz, R., Cohen, M.: Advan. At. Mol. Phys. **7**, 97 (1971)
6. Daudel, R., Stephens, M. E., Kapuy, E., Kozmutza, C.: Chem. Phys. Letters **40**, 194 (1976)
7. Robb, M. A., Haines, W. J., Csizmadia, I. G., J. Am. Chem. Soc. **95**, 42 (1973)
8. Daudel, R., Stephens, M. E., Kozmutza, C., Kapuy, E., Goddard, J. D., Csizmadia, I. G.: Intern. J. Quantum Chem. (accepted for publication)
9. Rényi, A.: Probability theory. Budapest: Akadémiai kiadó 1970
10. Interatomic distances suppl., Special Publication No. 18. London: The Chemical Society 1965
11. Daudel, R., Kozmutza, C., Kapuy, E.: Chem. Phys. Letters **36**, 555 (1975)
12. Gillespie, R. J.: Molecular geometry. London: Van Nostrand-Reinhold 1972

Received April 26, 1976